NEURAL NETWORK APPROXIMATION BASED ON HAUSDORFF DISTANCE OF TROPICAL ZONOTOPES

Anonymous authors
Paper under double-blind review

ABSTRACT

In this work we theoretically contribute to neural network approximation by providing a novel tropical geometrical viewpoint to structured neural network compression. In particular, we show that the approximation error over a bounded sphere of two neural networks with ReLU activations and one hidden layer depends on the Hausdorff distance of the respective zonotopes. This theorem comes as a first step towards a purely geometrical interpretation of neural network approximation. Based on this theoretical contribution, we propose geometrical methods that employ the K-means algorithm to compress the fully connected parts of ReLU activated deep neural networks. We analyze the error bounds of our algorithms theoretically based on our approximation theorem and evaluate them empirically on neural network compression. Our experiments follow a proof-of-concept strategy and indicate that our geometrical tools achieve improved performance over relevant tropical geometry techniques and can be competitive against non-tropical methods.

1 INTRODUCTION

Tropical geometry (Maclagan & Sturmfels, 2015) is a mathematical field based on algebraic geometry and strongly linked to polyhedral and combinatorial geometry. It is built upon the *tropical semiring* which originally refers to the min-plus semiring $(\mathbb{R}_{\text{min}}, \wedge, +)$, but may also refer to the max-plus semiring (Cuninghame-Green, 2012; Butkovič, 2010). In our work, we follow the convention of the max-plus semiring $(\mathbb{R}_{\text{max}}, \vee, +)$ which replaces the classical operations of addition and multiplication by max and sum respectively. These operations turn polynomials into piecewise linear functions and, thus, having direct applications in neural networks.

Tropical mathematics have a wide range of applications including game theory (Akian et al., 2012), dynamical systems on weighted lattices (Maragos, 2017), finite state transducers (Theodosis & Maragos, 2018; 2019) and convex regression (Maragos & Theodosis, 2020; Tsilivis et al., 2021). Recently, there has been remarkable theoretical impact of tropical geometry in the study of neural networks and machine learning (Maragos et al., 2021). Zhang et al. (2018) prove the equivalence of ReLU activated neural networks with tropical rational mappings. Furthermore, they show that zonotopes may serve as a computational mean for applications such as computing the bound shown in (Montúfar et al., 2014) regarding the number of the network's linear regions. In a similar context, Charisopoulos & Maragos (2018) compute an upper bound to the number of linear regions of convolutional and MaxOut layers and propose a randomized algorithm for linear region counting. Moreover, Charisopoulos & Maragos (2017) study the morphological perceptron tropically and propose a training algorithm using the convex-concave procedure. Also, Dimitriadis & Maragos (2021) examine the training, pruning and shape properties of Morphological neural networks.

Pruning (Blalock et al., 2020) or, generally, compressing neural networks gained interest in recent years due to the surprising capability of reducing the size of a neural network without compromising performance. As tropical geometry explains the mathematical structure of neural networks, pruning may be revisited tropically. Indeed, Alfarra et al. (2020) study the lottery ticket hypothesis (Frankle & Carbin, 2018) from the tropical geometrical perspective and propose an unstructured compression algorithm based sparsifying the zonotope matrices of the network. Further, Smyrnis et al. (2020) propose a novel tropical division algorithm that applies to neural network minimization. A generalization of this method applies to multiclass networks (Smyrnis & Maragos, 2020).

Contributions In our work, we contribute to structured neural network approximation from the mathematical viewpoint of tropical geometry:

- We establish a novel bound on the approximation error of two neural networks with ReLU activations and one hidden layer based on tropical geometry. To prove this we bound the error of two tropical polynomials via the Hausdorff distance of their respective Extended Newton Polytopes, which for the neural network case have the structure of zonotopes.
- Motivated by the geometrical bound, we derive two geometrical neural network compression methods that are based on zonotope reduction and employ K-means algorithm. Our algorithms are applied on the fully connected layers of ReLU activated neural networks.
- Our geometrical algorithms are analyzed both theoretically and experimentally. The theoretical evaluation is based on the bounding theorem of neural network approximation error by the Hausdorff distance of the zonotopes. On the experimental part, we examine the performance of our algorithms on retaining the accuracy of convolutional neural networks when applying compression on their fully connected layers.

Proofs, illustrations and experimental specifications are included in the supplementary material.

2 Background on Tropical Geometry

We study tropical geometry from the viewpoint of the *max-plus semiring* $(\mathbb{R}_{\max}, \vee, +)$ which is defined as the set $\mathbb{R}_{\max} = \mathbb{R} \cup \{-\infty\}$ equipped with two operations $(\vee, +)$. Operation $\vee$ stands for max and $+$ stands for sum. In max-plus algebra we define polynomials in the following way.

Tropical polynomials A *tropical polynomial* f in d variables $\mathbf{x} = (x_1, x_2, ..., x_d)^T$ is defined as the function

$$f(\mathbf{x}) = \max_{\mathbf{a} \in A} \{\mathbf{a}^T \mathbf{x} + c_{\mathbf{a}}\} \tag{1}$$

where A is a finite collection of vectors in $\mathbb{R}^d$ and $c_{\mathbf{a}}$ is the corresponding monomial coefficient in $\mathbb{R}_{\max} = \mathbb{R} \cup \{-\infty\}$. The set of such polynomials constitutes the semiring $\mathbb{R}_{\max}[\mathbf{x}]$ of tropical polynomials. Note that each term $\mathbf{a}^T\mathbf{x} + c_{\mathbf{a}}$ corresponds to a hyperplane in $\mathbb{R}^d$. We thus call the vectors $\mathbf{a} \in A$ the *slopes* of the tropical polynomial, and $c_{\mathbf{a}}$ the respective *bias*. We allow slopes to take any value in $\mathbb{R}^d$ and rather than $\mathbb{Z}^d_{\geq 0}$, as it is normally the case for regular polynomials. These polynomials are also referred to as *signomials* (Duffin & Peterson, 1973) in the literature.

Polytopes Polytopes have been studied extensively (Ziegler, 2012; Grünbaum, 2013) and occur as a geometric tool for fields such as linear programming and optimization. They also have an important role in the analysis of neural networks. For instance, Zhang et al. (2018); Charisopoulos & Maragos (2018) show that linear regions of neural networks correspond to vertices of polytopes. Thus, the counting of linear regions reduces to a combinatorial geometry problem. In what follows, we explore this connection of tropical geometry with polytopes.

Consider the tropical polynomial defined in (1). The *Newton Polytope* associated to $f(\mathbf{x})$ is defined as the convex hull of the slopes of the polynomial

$$\text{Newt}\,(f) := \text{conv}\{\mathbf{a} : \mathbf{a} \in A\}$$

Furthermore, the *Extended Newton Polytope* of $f(\mathbf{x})$ is defined as the convex hull of the slopes of the polynomial extended in the last dimension by the corresponding bias coefficient.

$$\text{ENewt}\,(f) := \text{conv}\{(\mathbf{a}^T,\, c_{\mathbf{a}}) : \mathbf{a} \in A\}$$

The following proposition computes the Extended Newton Polytope that occurs when a tropical operation is applied between two tropical polynomials. It will allow us to compute the polytope representation corresponding to a neural network's hidden layer.

Proposition 1. *(Zhang et al., 2018; Charisopoulos & Maragos, 2018) Let $f, g \in \mathbb{R}_{max}[\mathbf{x}]$ be two tropical polynomials . Then for the Extended Newton Polytopes it is true that*

$$\textit{ENewt}\,(f \vee g) = \textit{conv}\{\textit{ENewt}\,(f) \cup \textit{ENewt}\,(g)\}$$
$$\textit{ENewt}\,(f + g) = \textit{ENewt}\,(f) \oplus \textit{ENewt}\,(g)$$

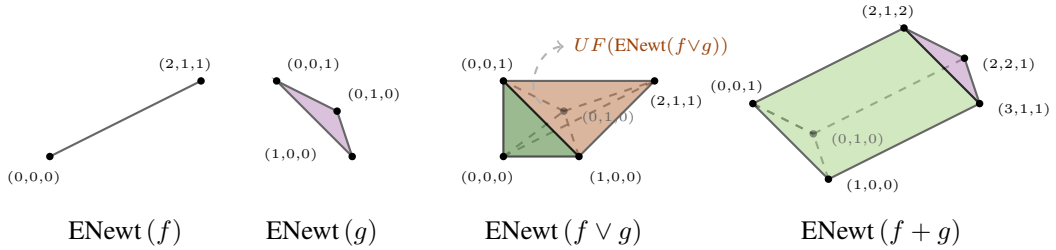

Figure 1: Illustration of tropical operations between polynomials. Max ($\vee$) corresponds to the convex hull of the union of points of the two Polytopes and sum ($+$) corresponds to Minkowski sum.

Here $\oplus$ denotes Minkowski addition. In particular, for two sets $A,\ B \subseteq \mathbb{R}^d$ it is defined as

$$A \oplus B := \{\mathbf{a} + \mathbf{b} \,|\, \mathbf{a} \in A, \mathbf{b} \in B\}$$

Corollary 1. *This result can be generalized to any finite set of polynomials using induction.*

Example 1. *Let f, g be two tropical polynomials in 2 variables, such that*

$$f(x, y) = \max(2x + y + 1, 0), \quad g(x, y) = \max(x, y, 1)$$

The tropical operations applied to these polynomials give

$$f \vee g = \max(2x + y + 1, 0, x, y, 1)$$
$$f + g = \max(3x + y + 1, x, 2x + 2y + 1, y, 2x + y + 2, 1)$$

Fig. 1 illustrates the Extended Newton Polytopes of the original and the computed polynomials.

The Extended Newton Polytope provides a geometrical representation of a tropical polynomial. In addition, it may be used to compute the values that the polynomial attains, as Proposition 2 indicates.

Proposition 2. *(Charisopoulos & Maragos, 2018) Let $f \in \mathbb{R}_{max}[\mathbf{x}]$ be a tropical polynomial in d variables. Let $UF\,(\text{ENewt}\,(f))$ be the points in the upper envelope of ENewt (f), where upward direction is taken regarding the last dimension of $\mathbb{R}^{d+1}$. Then for each $\mathbf{a} \in A$ there exists a linear region of f on which $f(\mathbf{x}) = \mathbf{a}^T\mathbf{x} + c_\mathbf{a}$ if and only if $(\mathbf{a}^T,\ c_\mathbf{a})$ is a vertex of $UF\,(\text{ENewt}\,(f))$.*

Example 2. *Using the polynomials from Example 1 we compute a reduced representation for $f \vee g$.*

$$f \vee g = \max(2x + y + 1, 0, x, y, 1) = \max(2x + y + 1, x, y, 1)$$

Indeed, the remaining terms correspond to the vertices of $UF(\text{ENewt}\,(f \vee g))$ shown in Fig. 1.

2.1 Tropical Geometry of Neural Networks

Tropical geometry has the capability of expressing the mathematical structure of ReLU activated neural networks. We review some of the basic properties governing neural networks and introduce notation that will be used in our analysis. For this purpose, consider the ReLU activated neural network of Fig. 2 with one hidden layer.

Network tropical equations The network consists of an *input layer* $\mathbf{x} = (x_1, ..., x_d)$, a *hidden layer* $f = (f_1, ..., f_n)$ with ReLU activations, an output layer $v = (v_1, ..., v_m)$ and two linear layers defined by the matrices A, C respectively. As illustrated in Fig. 2 we have $A_{i,:} = \left(\mathbf{a}_i^T,\ b_i\right)$ for the first linear layer and $C_{j,:} = (c_{j1}, c_{j2}, ..., c_{jn})$ for the second linear layer, as we ignore its biases. Furthermore, the output of the $i-$th component of the hidden layer f is computed as

$$f_i(\mathbf{x}) = \max\left(\sum_{k=1}^{d} a_{ik}x_k + b_i, 0\right) = \max(\mathbf{a}_i^T\mathbf{x} + b_i, 0) \tag{2}$$

We deduce that each f_i is a tropical polynomial with two terms. It therefore follows that ENewt (f_i) is a linear segment in $\mathbb{R}^{d+1}$. The components of the output layer may be computed as

$$v_j(\mathbf{x}) = \sum_{i=1}^{n} c_{ji}f_i(\mathbf{x}) = \sum_{c_{ji}>0} |c_{ji}|f_i(\mathbf{x}) - \sum_{c_{ji}<0} |c_{ji}|f_i(\mathbf{x}) = p_j(\mathbf{x}) - q_j(\mathbf{x}) \tag{3}$$

Tropical rational functions Functions p_j, q_j are both linear combinations of $\{f_i\}$ with positive coefficients, which implies that they are tropical polynomials. We conclude that every output node v_i can be written as a difference of two tropical polynomials, which is defined as a *tropical rational function*. This indicates that the output layer of the neural network of Fig. 2 is equivalent to a *tropical rational mapping*. In fact, this result holds for deeper networks, in general, as demonstrated by Theorem 1.

Theorem 1. *(Zhang et al., 2018) Consider a ReLU activated deep neural network as a mapping $F : \mathbb{R}^d \to \mathbb{R}^m$. Then F is equivalent to a tropical rational mapping.*

It is not known whether a tropical rational function $r(\mathbf{x})$ admits an efficient geometric representation that determines its values $\{r(\mathbf{x})\}$ for $\mathbf{x} \in \mathbb{R}^d$, as it holds for tropical polynomials with their polytopes in Proposition 2. For this reason, we choose to work separately on the polytopes of the tropical polynomials p_j, q_j.

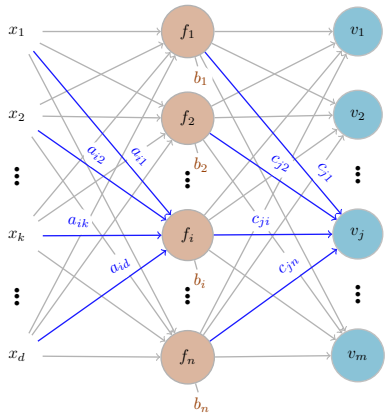

Figure 2: Neural network with one hidden ReLU layer. The first linear layer has weights $\{\mathbf{a}_i^T\}$ with bias $\{b_i\}$ corresponding to $i-$th node $\forall i \in [n]$ and the second has weights $\{c_{ji}\}, \forall j \in [m], i \in [n]$.

Zonotopes Zonotopes are defined as the Minkowski sum of a finite set of line segments. They are a special case of polytopes that occur as a building block for our network. These geometrical structures provide a representation of the polynomials p_j, q_j in (3) that further allows us to build our compression algorithms. We use the notation P_j, Q_j for the Extended Newton Polytopes of tropical polynomials p_j, q_j, respectively. Notice from (3) that for each component v_j of the output p_j, q_j are written as linear combinations of tropical polynomials that correspond to linear segments. Thus P_j and Q_j are zonotopes. We call P_j the *positive* zonotope, corresponding to the positive polynomial p_j and Q_j the *negative* one.

Zonotope Generators Each neuron of the hidden layer represents geometrically a line segment contributing to the positive or negative zonotope. We thus call these line segments *generators* of the zonotope. The generators further receive the characterization *positive* or *negative* depending on the zonotope they contribute to. It is intuitive to expect that a zonotope gets more complex as its number of generators increases. In fact, each vertex of the zonotope can be computed as the sum of vertices of the generators, where we choose a vertex from each generating line segment, either $\mathbf{0}$ or $c_{ji}\left(\mathbf{a}_i^T, b_i\right)$. We summarize the above with the following extension of (Charisopoulos & Maragos, 2018).

Proposition 3. *P_j, Q_j are zonotopes in $\mathbb{R}^{d+1}$. For each vertex $\mathbf{v}$ of P_j there exists a subset of indices I_+ of $\{1, 2, ..., n\}$ with $c_{ji} > 0$, $\forall i \in I_+$ such that $\mathbf{v} = \sum_{i \in I_+} c_{ji}\left(\mathbf{a}_i^T, b_i\right)$. Similarly, a vertex $\mathbf{u}$ of Q_j can be written as $\mathbf{u} = \sum_{i \in I_-} c_{ji}\left(\mathbf{a}_i^T, b_i\right)$ where I_- corresponds to $c_{ji} < 0$, $\forall i \in I_-$.*

3 Approximation of Tropical Polynomials

In this section we present the core theorem of our contribution that bounds the error of the approximation of two neural networks following the architecture of Fig. 2. To achieve this we first need to derive a bound on the error of approximating a simpler functional structure, namely tropical polynomials. The motivation behind the geometrical bounding of the error of the polynomials is Proposition 2. It indicates that a polynomial's values are determined at each point of the input space by the upper envelope of its Extended Newton Polytope. Therefore, it is expected that two tropical polynomials with approximately equal Extended Newton Polytopes, should attain similar values. We formally prove this intuitive result and the bound of the error depends on how close the corresponding Extended Newton Polytopes are. The metric we use to define this notion is the *Hausdorff distance*.

Hausdorff distance The distance of a point $\mathbf{u} \in \mathbb{R}^d$ from the finite set $\mathcal{V} \subset \mathbb{R}^d$ is denoted by either $\operatorname{dist}(\mathbf{u}, \mathcal{V})$ or $\operatorname{dist}(\mathcal{V}, \mathbf{u})$ and computed as $\min\{\|\mathbf{u} - \mathbf{v}\|,\ \mathbf{v} \in \mathcal{V}\}$ which is the Euclidean distance

of $\mathbf{u}$ from its closest point $\mathbf{v} \in \mathcal{V}$. The *Hausdorff distance* $\mathcal{H}(\mathcal{V},\mathcal{U})$ of two finite point sets $\mathcal{V},\mathcal{U} \subset \mathbb{R}^d$ is defined as

$$\mathcal{H}(\mathcal{V},\mathcal{U}) = \max\left\{\max_{\mathbf{v}\in\mathcal{V}} \operatorname{dist}(\mathbf{v},\mathcal{U}), \max_{\mathbf{u}\in\mathcal{U}} \operatorname{dist}(\mathcal{V},\mathbf{u})\right\}$$

Let $P, \tilde{P}$ be two polytopes with their vertex sets denoted by $\mathcal{V}_P, \mathcal{V}_{\tilde{P}}$ respectively. We define the Hausdorff distance $\mathcal{H}\left(P, \tilde{P}\right)$ of the two polytopes as the Hausdorff distance of their respective vertex sets $\mathcal{V}_P, \mathcal{V}_{\tilde{P}}$. Namely,

$$\mathcal{H}\left(P, \tilde{P}\right) := \mathcal{H}\left(\mathcal{V}_P, \mathcal{V}_{\tilde{P}}\right) \tag{4}$$

Clearly, the Hausdorff distance is a metric of how close two polytopes are to each other. Indeed, it becomes zero when the two polytopes coincide. According to this metric, the following bound on the error of tropical polynomial approximation is derived.

Proposition 4. *Let $p, \tilde{p} \in \mathbb{R}_{max}[\mathbf{x}]$ be two tropical polynomials and let $P = ENewt(p), \tilde{P} = ENewt(\tilde{p})$. Then,*

$$\max_{x\in\mathcal{B}} |p(\mathbf{x}) - \tilde{p}(\mathbf{x})| \leq \rho \cdot \mathcal{H}\left(P, \tilde{P}\right)$$

where $\mathcal{B} = \{\mathbf{x} \in \mathbb{R}^d : \|\mathbf{x}\| \leq r\}$ is the hypersphere of radius r, and $\rho = \sqrt{r^2+1}$.

The above proposition enable us to handle the more general case of neural networks with one hidden layer, that are equivalent with tropical rational mappings. Applying repeatedly Proposition 4 to each tropical polynomial corresponding to the networks, we get the following bound.

Theorem 2. *Let $v, \tilde{v} \in \mathbb{R}_{max}[\mathbf{x}]$ be two neural networks with architecture as in Fig. 2. With $\tilde{P}_j, \tilde{Q}_j$ we denote the positive and negative zonotopes of $\tilde{v}$. The following bound holds.*

$$\max_{x\in\mathcal{B}} \|v(\mathbf{x}) - \tilde{v}(\mathbf{x})\|_1 \leq \rho \cdot \left(\sum_{j=1}^{m} \mathcal{H}\left(P_j, \tilde{P}_j\right) + \mathcal{H}\left(Q_j, \tilde{Q}_j\right)\right)$$

Remark 1. The reason we choose to compute the error of the approximation on a bounded hypersphere $\mathcal{B}$ is twofold. Firstly, the unbounded error of linear terms always diverges to infinity and, secondly, in practice the working subspace of our dataset is usually bounded, e.g. images.

4 Neural Network Compression Algorithms

Compression problem formulation The tropical geometry theorem on the approximation of neural networks enables us to derive compression algorithms for ReLU activated neural networks. Suppose that we want to compress the neural network of Fig. 2 by reducing the number of neurons in the hidden layer, from n to K. Let us assume that the output of the compressed network is the tropical rational map $\tilde{v} = (\tilde{v}_1, ..., \tilde{v}_m)$. Its $j-$th component may be written as $\tilde{v}_j(\mathbf{x}) = \tilde{p}_j(\mathbf{x}) - \tilde{q}_j(\mathbf{x})$ where using Proposition 3 the zonotopes of $\tilde{p}_j, \tilde{q}_j$ are generated by $\tilde{c}_{ji}(\tilde{\mathbf{a}}_i^T, \tilde{b}_i)$, $\forall i$. The generators need to be chosen in such a way that $\tilde{v}_j(\mathbf{x}) \approx v_j(\mathbf{x})$ for all $\mathbf{x} \in \mathcal{B}$. Due to Theorem 2 it suffices to find generators such that the resulting zonotopes have $\mathcal{H}\left(P_j, \tilde{P}_j\right), \mathcal{H}\left(Q_j, \tilde{Q}_j\right)$ as small as possible $\forall j$. We thus formulated neural network compression as a geometrical zonotope approximation problem.

Our approaches Approximating a zonotope with fewer generators is a problem known as zonotope order reduction (Kopetzki et al., 2017). In our case we approach this problem by manipulating the zonotope generators $c_{ji}\left(\mathbf{a}_i^T, b_i\right), \forall i, j$ [1]. Each of the algorithms presented will create a subset of altered generators that approximate the original zonotopes. Ideally, we require the approximation to hold simultaneously for all positive and negative zonotopes of each output component v_j. However, this is not always possible, as in the case of multiclass neural networks, and it necessarily leads to heuristic manipulation. Our first attempt to tackle this problem applies the K-means algorithm to the

[1] Dealing with the full generated zonotope would lead to exponential computational overhead.

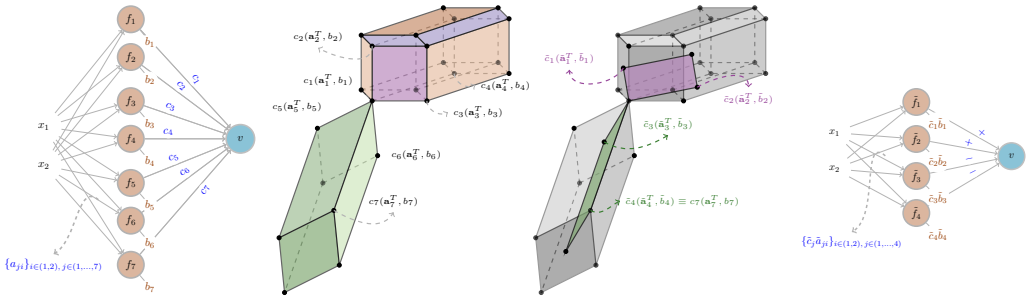

(a) Original network. (b) Original zonotopes (c) Resulting zonotopes. (d) Minimized network.

Figure 3: Illustration of Zonotope K-means execution. The original zonotope P is generated by $c_i\left(\mathbf{a}_i^T,\, b_i\right)$ for $i = 1, ..., 4$ and the negative zonotope Q generated by the remaining ones $i = 5, 6, 7$. The approximation $\tilde{P}$ of P is colored in purple and generated by $\tilde{c}_i\left(\tilde{\mathbf{a}}_i^T,\, \tilde{b}_i\right),\ i = 1, 2$ where the first generator is the K-means center representing the generators $1, 2$ of P and the second is the representative center of $3, 4$. Similarly, the approximation $\tilde{Q}$ of Q is colored in green and defined by the generators $\tilde{c}_i\left(\tilde{\mathbf{a}}_i^T,\, \tilde{b}_i\right),\ i = 3, 4$ that stand as representative centers for $\{5, 6\}$ and 7 respectively.

positive and negative generators, separately. This method is restricted on applying to single output neural networks. Our second approach further develops this technique to multiclass neural networks. Specifically, it utilizes K-means on the vectors associated with the Neural Paths passing from a node in the hidden layer, as we define later. The algorithms we present refer to the neural network of Fig. 2 with one hidden layer, but we may repeatedly apply them to compress deeper networks.

4.1 Zonotope Approximation

Zonotope K-means The first compression approach is geometrical and utilizes K-means, which is inherently a vector compression algorithm. Consider the case of a single output neural network, e.g as in Fig. 2 but with $m = 1$, and wish to reduce its hidden layer size from n to K neurons. We use the notation $c_i,\ i = 1, ..., n$ for weights of the second linear layer, connecting the hidden layer with the output node. Algorithm 1 is presented and an example of its execution can be found in Fig. 3.

Algorithm 1: Zonotope K-means Compression

1. Split generators into positive $\left\{c_i\left(\mathbf{a}_i^T,\, b_i\right) : c_i > 0\right\}$ and negative $\left\{c_i\left(\mathbf{a}_i^T,\, b_i\right) : c_i < 0\right\}$.
2. Apply K-means for $\frac{K}{2}$ centers, separately for both sets of generators and receive $\left\{\tilde{c}_i\left(\tilde{\mathbf{a}}_i^T,\, \tilde{b}_i\right) :\ \tilde{c}_i > 0\right\}, \left\{\tilde{c}_i\left(\tilde{\mathbf{a}}_i^T,\, \tilde{b}_i\right) :\ \tilde{c}_i < 0\right\}$ as output.
3. Construct the final weights. For the first linear layer, the weights and the bias which correspond to the $i-$th neuron become the vector $\tilde{c}_i\left(\tilde{\mathbf{a}}_i^T,\, \tilde{b}_i\right)$.
4. The weights of the second linear layer are set to 1 for every hidden layer neuron where $\tilde{c}_i\left(\tilde{\mathbf{a}}_i^T,\, \tilde{b}_i\right)$ occurs from positive generators and -1, elsewhere.

Proposition 5. *Zonotope K-means produces a compressed neural network with output $\tilde{v}$ satisfying*

$$\frac{1}{\rho} \cdot \max_{\mathbf{x} \in \mathcal{B}} |v(\mathbf{x}) - \tilde{v}(\mathbf{x})| \leq K \cdot \delta_{max} + \left(1 - \frac{1}{N_{max}}\right) \sum_{i=1}^{n} |c_i| \| \left(\mathbf{a}_i^T,\, b_i\right) \|$$

where K is the total number of centers used in both K-means, δ_{max} is the largest distance from a point to its corresponding cluster center and N_{max} is the maximum cardinality of a cluster.

The above proposition provides an upper bound for the approximation error of resulting network of Zonotope K-means from the original one. This bound increases as we use fewer cluster centers in

K-means. If we use $K \approx n$ centers the error approaches 0, because then $\delta_{\text{max}} \to 0, N_{\text{max}} \to 1$, and if $K \approx 0$ the error gets a fixed value depending on the magnitude of the weights of the linear layers.

4.2 MULTIPLE ZONOTOPE APPROXIMATION

The exact positive and negative zonotope approximation performed by Zonotope K-means algorithm has a main disadvantage: it can only be used in single output neural networks. Indeed, suppose that we want to employ the preceeding algorithm to approach the zonotopes of each output in a multiclass neural network. That would require $2m$ separate executions of K-means which are not necessarily consistent. For instance, it is possible to have $c_{j_1 i} > 0$ and $c_{j_2 i} < 0$ for some output components v_{j_1}, v_{j_2}. That means that in the compression procedure of v_{j_1}, the $i-$th neuron belongs to the positive generators set, while for v_{j_2}, it belongs to the negative one. This makes the two compressions incompatible. Moreover, the drawback of restricting to single output only allow us to compress the final ReLU layer and not any preceeding ones.

Algorithm 2: Neural Path K-means Compression

1. Apply K-means for K centers to the vectors $\left(\mathbf{a}_i^T,\, b_i,\, C_{:,i}^T\right)$, $i = 1, ..., n$, and get the centers $\left(\tilde{\mathbf{a}}_i^T,\, \tilde{b}_i,\, \tilde{C}_{:,i}^T\right)$, $i = 1, ..., K$.
2. Construct the final weights. For the first linear layer matrix the $i - th$ row becomes $\left(\tilde{\mathbf{a}}_i^T,\, \tilde{b}_i\right)$, while for the second linear layer matrix, the $i - th$ column becomes $\tilde{C}^{(i)}$.

Neural Path K-means To overcome this obstacle we apply a simultaneous approximation of the zonotopes. The method is called *Neural Path K-means* and directly applies K-means to the vectors of the weights $\left(\mathbf{a}_i^T,\, b_i,\, c_{1i},\, ...,\, c_{mi}\right)$ associated to each neuron i of the hidden layer. The name of the algorithm emanates from the fact that the vector associated to each neuron consists of the weights of all the neural network paths passing from this neuron. The procedure is presented in Algorithm 2.

Null Generators Neural Path K-means does not apply compression directly to each zonotope of the network, but is rather a heuristic approach for this task. Precisely, if we focus on the set of generators of the zonotopes of output j, Neural Path K-means might mix positive and negative generators together in the same cluster. For instance, suppose $\left(\tilde{\mathbf{a}}_k^T,\, \tilde{b}_k,\, \tilde{C}_{:,k}^T\right)$ is the cluster center corresponding to vectors $\left(\mathbf{a}_i^T,\, b_i,\, C_{:,i}^T\right)$ for $i \in I$. Then regarding output j, it is not necessary that $\forall i \in I$ all c_{ji} have the same sign. Thus, the compressed positive zonotope $\tilde{P}_j$ might contain generators of the original negative zonotope Q_j and vice versa. We will call generators $c_{ji}\left(\mathbf{a}_i^T,\, b_i\right)$ contributing to opposite zonotopes, *null generators*.

Proposition 6. *Neural Path K-means produces a compressed neural network with output $\tilde{v}$ satisfying*

$$\frac{1}{\rho} \cdot \sum_{j=1}^{m} \max_{\mathbf{x} \in \mathcal{B}} |v_j(\mathbf{x}) - \tilde{v}_j(\mathbf{x})| \leq \sqrt{m} K \delta_{max}^2 + \sqrt{m}\left(1 - \frac{1}{N_{max}}\right) \sum_{i=1}^{n} \|C_{:,i}\| \left\|\left(\mathbf{a}_i^T,\, b_i\right)\right\| + \frac{\sqrt{m}\delta_{max}}{N_{min}} \sum_{i=1}^{n} \left(\left\|\left(\mathbf{a}_i^T,\, b_i\right)\right\| + \|C_{:,i}\|\right) + \sum_{j=1}^{m} \sum_{i \in \mathcal{N}_j} |c_{ji}| \left\|\left(\mathbf{a}_i^T,\, b_i\right)\right\|$$

where K is the number of K-means clusters, δ_{max} the maximum distance from any point to its corresponding cluster center, N_{max}, N_{min} the maximum and minimum cardinality respectively of a cluster and $\mathcal{N}_j$ the set of null generators with respect to output j.

The performance of Neural Path K-means is evaluated with Proposition 6. The result we deduce is analogous to Zonotope K-means. The approximation error is eliminated as the number K of centers approaches n. This holds because for $K = n$ we get $\delta_{\text{max}} = 0$, $N_{\text{max}} = 1$ and $\mathcal{N}_j = \emptyset$, $\forall j \in [m]$. However, as K is reduced, the upper bound reaches a value depending on the magnitude of the weights of the linear layers together with weights corresponding to null generators.

Table 1: Reporting accuracy of compressed networks for single output compression methods.

Percentage of Remaining Neurons	MNIST $3/5$			MNIST $4/9$		
	(Smyrnis et al., 2020)	Zonotope K-means	Neural Path K-means	(Smyrnis et al., 2020)	Zonotope K-means	Neural Path K-means
100% (Original)	99.18 ± 0.27	99.38 ± 0.09	99.38 ± 0.09	99.53 ± 0.09	99.53 ± 0.09	99.53 ± 0.09
5%	99.12 ± 0.37	99.42 ± 0.07	99.25 ± 0.04	98.99 ± 0.09	99.52 ± 0.09	99.48 ± 0.15
1%	99.11 ± 0.36	99.39 ± 0.05	99.32 ± 0.03	99.01 ± 0.09	99.46 ± 0.05	99.35 ± 0.17
0.5%	99.18 ± 0.36	99.41 ± 0.05	99.22 ± 0.11	98.81 ± 0.09	99.35 ± 0.24	98.84 ± 1.18
0.3%	99.18 ± 0.36	99.25 ± 0.37	99.19 ± 0.41	98.81 ± 0.09	98.22 ± 1.38	98.22 ± 1.33

Table 2: Reporting theoretical upper bounds of Propositions 5, 6.

Percentage of Remaining Neurons	MNIST $3/5$		MNIST $4/9$	
	Zonotope K-means	Neural Path K-means	Zonotope K-means	Neural Path K-means
100%	0.00	0.00	0.00	0.00
10%	17.07	246.74	18.85	229.37
2.5%	15.35	59.42	17.02	63.37
1%	14.79	42.22	16.44	45.58
0.5%	14.57	36.47	16.20	39.71

5 EXPERIMENTS

We conduct experiments on compressing the linear layers of convolutional neural networks, while leaving the convolutional filters unchanged. Our experiments work as a proof-of-concept indicating that our theoretical claims indeed hold in practice. In particular, the heart of our contribution lies in presenting novel tropical geometrical background for neural network compression. Moreover, our techniques motivate further research in the area, which will allow them to become more competitive.

Our methods compress the linear layers of the network layer by layer. They perform a functional approximation of the original network and thus they are applicable for both classification and regression tasks. To compare them with other techniques in the literature we choose methods with similar structure, i.e. structured pruning techniques without re-training. For example, Alfarra et al. (2020) propose a compression algorithm based on the sparsification of the matrices representing the zonotopes and worked as a great intuition for our work. However, their method is unstructured and incompatible for comparison. The methods we choose to compare are two tropical methods for single-output (Smyrnis et al., 2020) and multi-output (Smyrnis & Maragos, 2020) networks, Random Structured, $L1$ and a modification of ThiNet (Luo et al., 2017) adapted to linear layers. Smyrnis et al. (2020); Smyrnis & Maragos (2020) propose a novel tropical division framework that aims on the reduction of zonotope vertices. Random method prunes neurons according to uniform probability, while $L1$ prunes those with the lowest value of $L1$ norm of their weights. Also, ThiNet uses a greedy criterion for discarding the neurons that have the smallest contribution to the output of the network.

MNIST Dataset, Pairs 3-5 and 4-9 The first experiment is performed on the binary classification tasks of pairs $3/5$ and $4/9$ of the MNIST dataset and so we can utilize both of our proposed methods. In Table 1, we compare our methods with a tropical geometrical approach of Smyrnis et al. (2020). Their method is based on a tropical division framework for network minimization. For fair comparison, we use the same CNN with two fully connected layers and hidden layer of size 1000. According to Table 1, our techniques seem to have similar performance. They retain the accuracy of the network while reducing its size. Moreover, in Table 2 we include experimental computation of the theoretical bounds provided by Proposition 5, 6. We notice that the bounds decrease as the remaining weights get less. The behaviour of the bounds was expected to be incremental because the less weights we use, the compression gets worse and the error becomes larger. However, the opposite holds which means that the bounds are tighter for higher pruning rates. It is also important to mention that the bounds become 0 when we keep all the weights, as expected.

MNIST and Fashion-MNIST Datasets For the second experiment we employ MNIST and Fashion-MNIST datasets. The corresponding classification is multiclass and thus Neural Path K-means may only be applied. In Table 3, we compare it with the multiclass tropical method of

Table 3: Reporting accuracy of compressed networks for multiclass compression methods.

Percentage of Remaining Neurons	MNIST		Fashion-MNIST	
	(Smyrnis & Maragos, 2020)	Neural Path K-means	(Smyrnis & Maragos, 2020)	Neural Path K-means
100% (Original)	98.60 $\pm$ 0.03	98.61 $\pm$ 0.11	88.66 $\pm$ 0.54	89.52 $\pm$ 0.19
50%	96.39 $\pm$ 1.18	98.13 $\pm$ 0.28	83.30 $\pm$ 2.80	88.22 $\pm$ 0.32
25%	95.15 $\pm$ 2.36	98.42 $\pm$ 0.42	82.22 $\pm$ 2.85	86.67 $\pm$ 1.12
10%	93.48 $\pm$ 2.57	96.89 $\pm$ 0.55	80.43 $\pm$ 3.27	86.04 $\pm$ 0.94
5%	92.93 $\pm$ 2.59	96.31 $\pm$ 1.29	–	83.68 $\pm$ 1.06

Smyrnis & Maragos (2020) using the same CNN architecture they do. Furthermore, in plots 4a, 4b we compare Neural Path K-means with ThiNet and baseline pruning methods by compressing LeNet5 (LeCun et al., 1998). To get a better idea of how our method performs in deeper architectures we provide plots 4c,4d that illustrate the performance of compressing a deep neural network with layers of size $28 * 28$, 512, 256, 128 and 10, which we refer to as deepNN. The compression is executed on all hidden layers beginning from the input and heading to the output. From Table 3, we deduce that our method performs better than (Smyrnis & Maragos, 2020). Also, it achieves higher accuracy scores and experience lower variance as shown in plots 4a-4d. Neural Path K-means, overall, seems to have good performance, even competitive to ThiNet. Its worst performance occurs on low percentages of remaining weights. An explanation for this is that K-means provides a high-quality compression as long as the number of centers is not less than the number of "real" clusters.

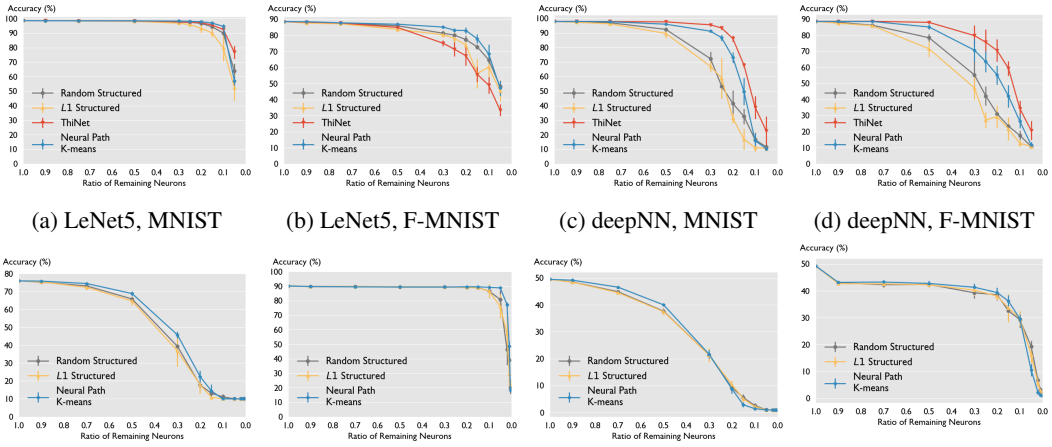

(a) LeNet5, MNIST (b) LeNet5, F-MNIST (c) deepNN, MNIST (d) deepNN, F-MNIST

(e) AlexNet, CIFAR10 (f) CIFAR-VGG, CIFAR10 (g) AlexNet, CIFAR100 (h) CIFAR-VGG, CIFAR100

Figure 4: Neural Path K-means compared with baseline pruning methods and ThiNet. Horizontal axis shows the ratio of remaining neurons in each hidden layer of the fully connected part.

CIFAR Dataset We conduct our final experiment on CIFAR datasets using CIFAR-VGG (Blalock et al., 2020) and an altered version of AlexNet adapted for CIFAR. The resulting plots are shown in Fig. 4e-4h. We deduce that Neural Path K-means retains a good performance on larger datasets. In particular, in most cases it has slightly better accuracy an lower deviation than the baselines, but has worse behaviour when keeping almost zero weights.

6 Conclusions and Future Work

We presented a novel theorem on the bounding of the approximation error of two neural networks with one hidden layer. This theorem occurs from the bounding of two tropical polynomials via the Hausdorff distance of their Extended Newton Polytopes. Our theorem can be used to derive geometrical compression algorithms for the fully connected part of ReLU activated deep neural networks, with application to convolutional layers being an ongoing work.

REFERENCES

Marianne Akian, Stéphane Gaubert, and Alexander Guterman. Tropical polyhedra are equivalent to mean payoff games. *International Journal of Algebra and Computation*, 22(01):1250001, 2012.

Motasem Alfarra, Adel Bibi, Hasan Hammoud, Mohamed Gaafar, and Bernard Ghanem. On the decision boundaries of deep neural networks: A tropical geometry perspective. *arXiv preprint arXiv:2002.08838*, 2020.

Davis Blalock, Jose Javier Gonzalez Ortiz, Jonathan Frankle, and John Guttag. What is the state of neural network pruning? *arXiv preprint arXiv:2003.03033*, 2020.

Peter Butkovič. *Max-linear systems: theory and algorithms*. Springer monographs in mathematics. Springer, 2010. ISBN 978-1-84996-298-8.

Vasileios Charisopoulos and Petros Maragos. Morphological perceptrons: geometry and training algorithms. In *International Symposium on Mathematical Morphology and Its Applications to Signal and Image Processing*, pp. 3–15. Springer, 2017.

Vasileios Charisopoulos and Petros Maragos. A tropical approach to neural networks with piecewise linear activations. *arXiv preprint arXiv:1805.08749*, 2018.

Raymond A Cuninghame-Green. *Minimax algebra*, volume 166. Springer Science & Business Media, 2012.

Nikolaos Dimitriadis and Petros Maragos. Advances in morphological neural networks: Training, pruning and enforcing shape constraints. In *Proc. 46th IEEE Int'l Conf. Acoustics, Speech and Signal Processing (ICASSP-2021)*, Toronto, June 2021.

Richard James Duffin and Elmor L Peterson. Geometric programming with signomials. *Journal of Optimization Theory and Applications*, 11(1):3–35, 1973.

Jonathan Frankle and Michael Carbin. The lottery ticket hypothesis: Finding sparse, trainable neural networks. *arXiv preprint arXiv:1803.03635*, 2018.

Branko Grünbaum. *Convex polytopes*, volume 221. Springer Science & Business Media, 2013.

Anna-Kathrin Kopetzki, Bastian Schürmann, and Matthias Althoff. Methods for order reduction of zonotopes. In *2017 IEEE 56th Annual Conference on Decision and Control (CDC)*, pp. 5626–5633. IEEE, 2017.

Yann LeCun, Léon Bottou, Yoshua Bengio, and Patrick Haffner. Gradient-based learning applied to document recognition. *Proceedings of the IEEE*, 86(11):2278–2324, 1998.

Jian-Hao Luo, Jianxin Wu, and Weiyao Lin. ThiNet: A Filter Level Pruning Method for Deep Neural Network Compression. In *2017 IEEE International Conference on Computer Vision (ICCV)*, pp. 5068–5076, 2017. doi: 10.1109/ICCV.2017.541.

Diane Maclagan and Bernd Sturmfels. *Introduction to tropical geometry*, volume 161. American Mathematical Soc., 2015.

Petros Maragos. Dynamical systems on weighted lattices: general theory. *Mathematics of Control, Signals, and Systems*, 29(4):1–49, 2017.

Petros Maragos and Emmanouil Theodosis. Multivariate tropical regression and piecewise-linear surface fitting. In *ICASSP 2020-2020 IEEE International Conference on Acoustics, Speech and Signal Processing (ICASSP)*, pp. 3822–3826. IEEE, 2020.

Petros Maragos, Vasileios Charisopoulos, and Emmanouil Theodosis. Tropical geometry and machine learning. *Proceedings of the IEEE*, 109(5):728–755, 2021. doi: 10.1109/JPROC.2021.3065238.

Guido Montúfar, Razvan Pascanu, Kyunghyun Cho, and Yoshua Bengio. On the number of linear regions of deep neural networks. *arXiv preprint arXiv:1402.1869*, 2014.

Georgios Smyrnis and Petros Maragos. Multiclass neural network minimization via tropical newton polytope approximation. In *Proc. Int'l Conf. on Machine Learning, PMLR*, 2020.

Georgios Smyrnis, Petros Maragos, and George Retsinas. Maxpolynomial division with application to neural network simplification. In *ICASSP 2020-2020 IEEE International Conference on Acoustics, Speech and Signal Processing (ICASSP)*, pp. 4192–4196. IEEE, 2020.

Emmanouil Theodosis and Petros Maragos. Analysis of the viterbi algorithm using tropical algebra and geometry. In *2018 IEEE 19th International Workshop on Signal Processing Advances in Wireless Communications (SPAWC)*, pp. 1–5. IEEE, 2018.

Emmanouil Theodosis and Petros Maragos. Tropical modeling of weighted transducer algorithms on graphs. In *ICASSP 2019 - 2019 IEEE International Conference on Acoustics, Speech and Signal Processing (ICASSP)*, pp. 8653–8657, 2019. doi: 10.1109/ICASSP.2019.8683127.

Nikos Tsilivis, Anastasios Tsiamis, and Petros Maragos. Sparsity in max-plus algebra and applications in multivariate convex regression. In *Proc. 46th IEEE Int'l Conf. Acoustics, Speech and Signal Processing (ICASSP-2021)*, Toronto, June 2021.

Liwen Zhang, Gregory Naitzat, and Lek-Heng Lim. Tropical geometry of deep neural networks. In *International Conference on Machine Learning*, pp. 5824–5832. PMLR, 2018.

Günter M Ziegler. *Lectures on polytopes*, volume 152. Springer Science & Business Media, 2012.

A PROOFS FOR THE SECTION "BACKGROUND ON TROPICAL GEOMETRY"

A.1 PROOF OF PROPOSITION 3

Proof. The first argument follows from the fact that both p_j, q_j are linear combinations of tropical polynomials consisting of two terms. Indeed, we compute

$$p_j(\mathbf{x}) = \sum_{c_{ji}>0} c_{ji} \max(\mathbf{a}_i^T \mathbf{x} + b_i, 0) = \sum_{c_{ji}>0} \max(c_{ji}\mathbf{a}_i^T \mathbf{x} + c_{ji} b_i, 0) \xrightarrow{\text{Prop. 1}}$$
$$P_j = \bigoplus_{c_{ji}>0} \text{ENewt}\left(\max(c_{ji}\mathbf{a}_i^T \mathbf{x} + c_{ji} b_i, 0)\right)$$

Each ENewt $\left(\max(c_{ji}\mathbf{a}_i^T \mathbf{x} + c_{ji} b_i, 0)\right)$ is a line segment with endpoints $\mathbf{0}$ and $\left(c_{ji}\mathbf{a}_i^T,\, c_{ji} b_i\right) = c_{ji}\left(\mathbf{a}_i^T,\, b_i\right)$. Therefore P_j is written as the Minkowski sum of line segments, which is a zonotope by definition. Similarly Q_j is a zonotope.

Furthermore, from the definition of the Minkowski sum, each point $\mathbf{v} \in P_j$ may be written as $\sum_{c_{ji}>0} \mathbf{v}_i$, where each $\mathbf{v}_i$ is a point in the segment ENewt $\left(\max(c_{ji}\mathbf{a}_i^T \mathbf{x} + c_{ji} b_i, 0)\right)$. A vertex of P_j can only occur if $\mathbf{v}_i$ is an extreme point of ENewt $\left(\max(c_{ji}\mathbf{a}_i^T \mathbf{x} + c_{ji} b_i, 0)\right)$ for every i which is equivalent to either $\mathbf{v}_i = \mathbf{0}$ or $\mathbf{v}_i = c_{ji}\left(\mathbf{a}_i^T,\, b_i\right)$. This means that every vertex of P_j corresponds to a subset $I_+ \subseteq [n]$ of indices i with $c_{ji} > 0$, for which we choose $\mathbf{v}_i = c_{ji}\left(\mathbf{a}_i^T,\, b_i\right)$ and for the rest it holds $\mathbf{v}_i = \mathbf{0}$. Thus,

$$\mathbf{v} = \sum_{i \in I_+} c_{ji}\left(\mathbf{a}_i^T,\, b_i\right)$$

In the same way we derive the analogous result for the negative zonotope Q_j. □

Corollary 2. *The geometric result concerning the structure of zonotopes can be extended to max-pooling layers. For instance, a max-pooling layer of size 2×2 corresponds to a polytope that is constructed as the Minkowski sum of pyramids which could stand as generalized case of zonotope.*

B PROOFS FOR THE SECTION "APPROXIMATION OF TROPICAL POLYNOMIALS"

B.1 PROOF OF PROPOSITION 4

Proof. Consider a point $\mathbf{x} \in \mathcal{B}$ and assume that $p(\mathbf{x}) = \mathbf{a}^T\mathbf{x} + b$, $\tilde{p}(\mathbf{x}) = \mathbf{c}^T\mathbf{x} + d$. Then,

$$p(\mathbf{x}) - \tilde{p}(\mathbf{x}) = p(\mathbf{x}) - \max_{(\tilde{\mathbf{a}}^T, \tilde{b}) \in \mathcal{V}_{\tilde{p}}} \{\tilde{\mathbf{a}}^T\mathbf{x} + \tilde{b}\} \leq \mathbf{a}^T\mathbf{x} + b - \left(\mathbf{u}^T,\, v\right)\begin{pmatrix}\mathbf{x}\\ 1\end{pmatrix}$$

where $\left(\mathbf{u}^T, v\right)$ may be any vertex of $\tilde{P}$. Similarly, we derive

$$\left(\mathbf{r}^T,\, s\right)\begin{pmatrix}\mathbf{x}\\ 1\end{pmatrix} - \left(\mathbf{c}^T\mathbf{x} + d\right) \leq p(\mathbf{x}) - \tilde{p}(\mathbf{x})$$

for any vertex $\left(\mathbf{r}^T, s\right)$ of P. Therefore, we may select the vertices $\left(\mathbf{u}^T, v\right) \in \tilde{P}$, $\left(\mathbf{r}^T, s\right) \in P$ so that their respective distances from $\left(\mathbf{a}^T, b\right)$ and $\left(\mathbf{c}^T, d\right)$, respectively, are minimized. Choosing them in such a way gives

$$\begin{aligned} p(\mathbf{x}) - \tilde{p}(\mathbf{x}) &\leq \mathbf{a}^T\mathbf{x} + b - \left(\mathbf{u}^T,\, v\right)\begin{pmatrix}\mathbf{x}\\ 1\end{pmatrix} = \left(\left(\mathbf{a}^T,\, b\right) - \left(\mathbf{u}^T,\, v\right)\right)\begin{pmatrix}\mathbf{x}\\ 1\end{pmatrix} \leq \\ &\leq \left\|\left(\mathbf{a}^T,\, b\right) - \left(\mathbf{u}^T,\, v\right)\right\| \left\|\begin{pmatrix}\mathbf{x}\\ 1\end{pmatrix}\right\| \leq d\left(\left(\mathbf{a}^T,\, b\right), \tilde{P}\right)\sqrt{r^2+1} \end{aligned} \tag{5}$$

In similar manner we deduce

$$\begin{aligned} p(\mathbf{x}) - \tilde{p}(\mathbf{x}) &\geq \left(\mathbf{r}^T,\, s\right)\begin{pmatrix}\mathbf{x}\\ 1\end{pmatrix} - \mathbf{c}^T\mathbf{x} + d = \left(\left(\mathbf{r}^T,\, s\right) - \left(\mathbf{c}^T,\, d\right)\right)\begin{pmatrix}\mathbf{x}\\ 1\end{pmatrix} \geq \\ &\geq -\left\|\left(\mathbf{r}^T,\, s\right) - \left(\mathbf{c}^T,\, d\right)\right\| \left\|\begin{pmatrix}\mathbf{x}\\ 1\end{pmatrix}\right\| \geq -d\left(P, \left(\mathbf{c}^T,\, d\right)\right)\sqrt{r^2+1} \end{aligned} \tag{6}$$

Notice, that for the relations (5) and (6) we used Cauchy-Schwartz inequality

$$|\langle \mathbf{x}, \mathbf{y} \rangle| \leq \|\mathbf{x}\|\|\mathbf{y}\| \Leftrightarrow -\|\mathbf{x}\|\|\mathbf{y}\| \leq \langle \mathbf{x}, \mathbf{y} \rangle \leq \|\mathbf{x}\|\|\mathbf{y}\|$$

Inequality (5) holds at any point $x \in \mathcal{B}$ for some vertex $\left(a^T,\, b\right) \in P$, therefore

$$p(\mathbf{x}) - \tilde{p}(\mathbf{x}) \leq \rho \cdot \max_{(\mathbf{a}^T, b) \in \mathcal{V}_P} d\left(\left(\mathbf{a}^T,\, b\right), \mathcal{V}_{\tilde{P}}\right) \tag{7}$$

for all $x \in \mathcal{B}$. Similarly, we derive

$$p(\mathbf{x}) - \tilde{p}(\mathbf{x}) \geq \min_{(\mathbf{c}, d) \in \mathcal{V}_{\tilde{P}}} -\rho \cdot d\left(\mathcal{V}_P, \left(\mathbf{c}^T,\, d\right)\right) = -\max_{(\mathbf{c}^T, d) \in \mathcal{V}_{\tilde{P}}} \rho \cdot d\left(\mathcal{V}_P, \left(\mathbf{c}^T,\, d\right)\right) \tag{8}$$

Combining (7) and (8) gives

$$-\max_{(\mathbf{c}^T, d) \in \mathcal{V}_{\tilde{P}}} \rho \cdot d\left(\mathcal{V}_P, \left(\mathbf{c}^T,\, d\right)\right) \leq p(\mathbf{x}) - \tilde{p}(\mathbf{x}) \leq \max_{(\mathbf{a}^T, b) \in \mathcal{V}_P} \rho \cdot d\left(\left(\mathbf{a}^T,\, b\right), \mathcal{V}_{\tilde{P}}\right) \Leftrightarrow$$

$$|p(\mathbf{x}) - \tilde{p}(\mathbf{x})| \leq \rho \cdot \max\left\{\max_{(\mathbf{a}^T, b) \in \mathcal{V}_P} \rho \cdot d\left(\left(\mathbf{a}^T,\, b\right), \mathcal{V}_{\tilde{P}}\right), \max_{(\mathbf{c}^T, d) \in \mathcal{V}_{\tilde{P}}} \rho \cdot d\left(\mathcal{V}_P, \left(\mathbf{c}^T,\, d\right)\right)\right\}$$

Hence, from the definition of the Hausdorff distance of two polytopes we derive the desired upper bound

$$|p(\mathbf{x}) - \tilde{p}(\mathbf{x})| \leq \rho \cdot \mathcal{H}\left(P, \tilde{P}\right),\ \forall \mathbf{x} \in \mathcal{B} \Rightarrow$$

$$\max_{\mathbf{x} \in \mathcal{B}} |p(\mathbf{x}) - \tilde{p}(\mathbf{x})| \leq \rho \cdot \mathcal{H}\left(P, \tilde{P}\right)$$

□

Remark 2. Note that with similar proof one may replace the Hausdorff distance of the two polytopes by the Hausdorff distance of their upper envelopes. This makes our theorem an exact generalization of Proposition 2. However, this format is difficult to use in practice, because it is computationally harder to determine the vertices of the upper envelope.

B.2 Proof of Theorem 2

Proof. Notice that we may write

$$\begin{aligned}\|v(\mathbf{x}) - \tilde{v}(\mathbf{x})\|_1 &= \sum_{j=1}^{m} |v_j(\mathbf{x}) - \tilde{v}_j(\mathbf{x})| = \sum_{j=1}^{m} |(p_j(\mathbf{x}) - q_j(\mathbf{x})) - (\tilde{p}_j(\mathbf{x}) - \tilde{q}_j(\mathbf{x}))| \\ &= \sum_{j=1}^{m} |(p_j(\mathbf{x}) - \tilde{p}_j(\mathbf{x})) - (q_j(\mathbf{x}) - \tilde{q}_j(\mathbf{x}))| \leq \sum_{j=1}^{m} |p_j(\mathbf{x}) - \tilde{p}_j(\mathbf{x})| + |q_j(\mathbf{x}) - \tilde{q}_j(\mathbf{x})|\end{aligned}$$

Thus from from Proposition 4 we derive

$$\max_{\mathbf{x} \in \mathcal{B}} \|v(\mathbf{x}) - \tilde{v}(\mathbf{x})\|_1 \leq \rho \cdot \left(\sum_{j=1}^{m} \mathcal{H}\left(P_j, \tilde{P}_j\right) + \mathcal{H}\left(Q_j, \tilde{Q}_j\right)\right)$$

□

C Proofs and Figures for the section "Neural Network Compression Algorithms"

C.1 Illustration of Zonotope K-means

Below we present a larger version of Fig. 5 demonstrating the execution of Zonotope K-means .

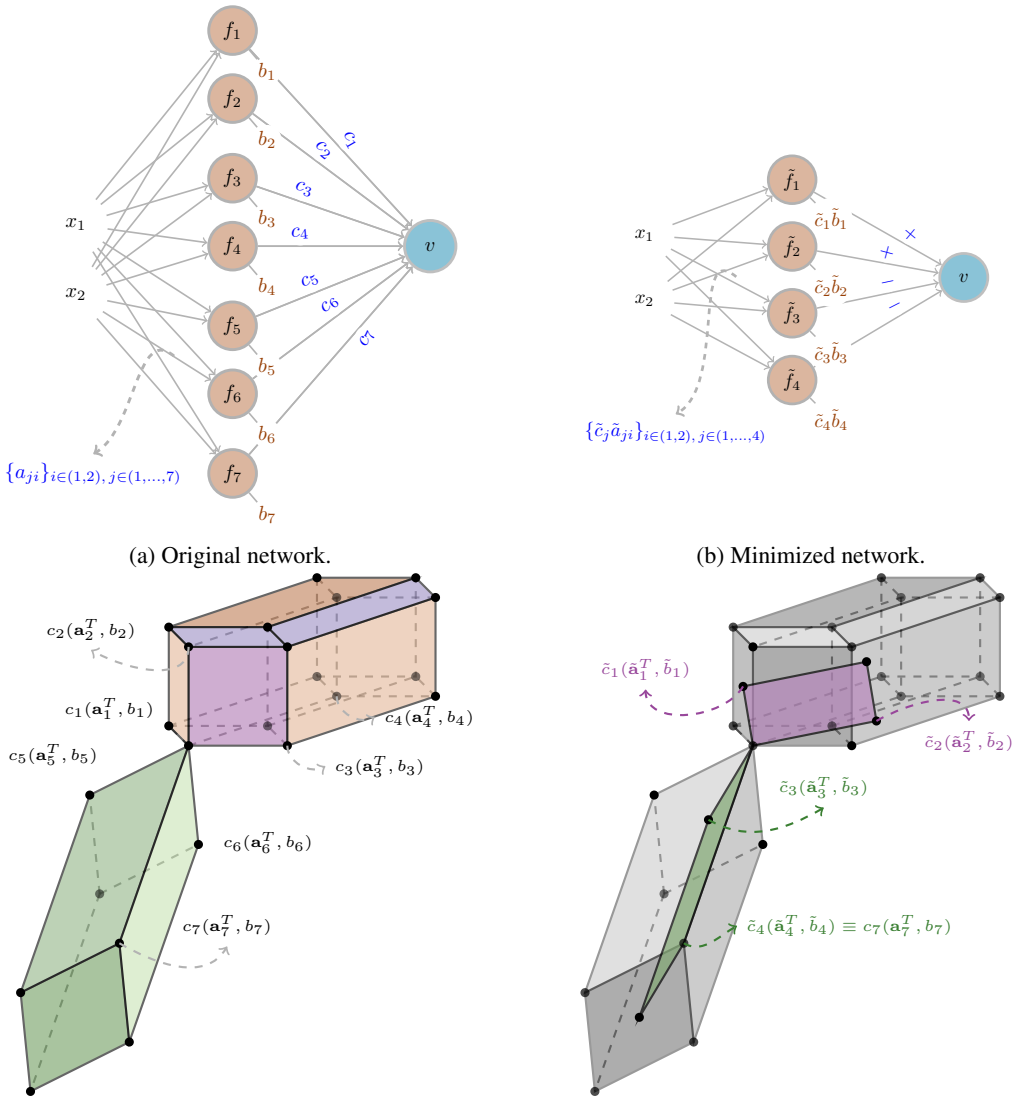

(a) Original network.

(b) Minimized network.

(c) Original zonotopes

(d) Approximating zonotopes.

Figure 5: Illustration of Zonotope K-means execution. The original zonotope P is generated by $c_i\left(\mathbf{a}_i^T,\, b_i\right)$ for $i = 1, ..., 4$ and the negative zonotope Q generated by the remaining ones $i = 5, 6, 7$. The approximation $\tilde{P}$ of P is colored in purple and generated by $\tilde{c}_i\left(\tilde{\mathbf{a}}_i^T,\, \tilde{b}_i\right)$, $i = 1, 2$ where the first generator is the K-means center representing the generators $1, 2$ of P and the second is the representative center of $3, 4$. Similarly, the approximation $\tilde{Q}$ of Q is colored in green and defined by the generators $\tilde{c}_i\left(\tilde{\mathbf{a}}_i^T,\, \tilde{b}_i\right)$, $i = 3, 4$ that stand as representative centers for $\{5, 6\}$ and 7 respectively.

C.2 Proof of Proposition 5

Proof. We remind that for the output functions it holds

$$v(\mathbf{x}) = p(\mathbf{x}) - q(\mathbf{x})\ ,\tilde{v}(\mathbf{x}) = \tilde{p}(\mathbf{x}) - \tilde{q}(\mathbf{x})$$

From triangle inequality we deduce

$$|v(\mathbf{x}) - \tilde{v}(\mathbf{x})| = |p(\mathbf{x}) - q(\mathbf{x}) - (\tilde{p}(\mathbf{x}) - \tilde{q}(\mathbf{x}))| < |p(\mathbf{x}) - \tilde{p}(\mathbf{x})| + |q(\mathbf{x}) - \tilde{q}(\mathbf{x})|$$

Prop 4 bounds $|p(\mathbf{x}) - \tilde{p}(\mathbf{x})|$ and $|q(\mathbf{x}) - \tilde{q}(\mathbf{x})|$ are bounded by $\mathcal{H}\left(P, \tilde{P}\right)$ and $\mathcal{H}\left(Q, \tilde{Q}\right)$ respectively. Therefore, it suffices to get an upper bound for these Hausdorff distances. Let us consider any

vertex $\mathbf{u} = \sum_{i \in I_+} c_i \left(\mathbf{a}_i^T,\, b_i\right)$ of P. For the vertex $\mathbf{u} \in P$ we need to choose vertex $\mathbf{v} \in \tilde{P}$ as close to $\mathbf{u}$ as possible, in order to provide an upper bound for $\operatorname{dist}\left(\mathbf{u}, \tilde{P}\right)$. Vertex $\mathbf{v}$ is selected as follows. For each $i \in I_+$ we select k such that $\tilde{c}_k \left(\tilde{\mathbf{a}}_k^T \quad \tilde{b}_k\right)$ is the center of the cluster where $c_i \left(\mathbf{a}_i^T,\, b_i\right)$ belongs to. We denote the set of such clusters by C_+, where each cluster center k appears only once. Then, vertex $\mathbf{v}$ is constructed as $\mathbf{v} = \sum_{k \in C_+} \tilde{c}_k \left(\tilde{\mathbf{a}}_k^T \quad \tilde{b}_k\right) \in \tilde{P}$. We have that:

$$
\begin{aligned}
\operatorname{dist}\left(\mathbf{u}, \tilde{P}\right) &\leq \left\| \sum_{i \in I_+} c_i \left(\mathbf{a}_i^T,\, b_i\right) - \sum_{k \in C_+} \tilde{c}_k \left(\tilde{\mathbf{a}}_k^T,\, \tilde{b}_k\right) \right\| \\
&\leq \sum_{k \in C_+} \left\| \sum_{i \in I_{k_+}} c_i \left(\mathbf{a}_i^T,\, b_i\right) - \tilde{c}_k \left(\tilde{\mathbf{a}}_k^T,\, \tilde{b}_k\right) \right\| \\
&\leq \sum_{k \in C_+} \sum_{i \in I_{k_+}} \left\| c_i \left(\mathbf{a}_i^T,\, b_i\right) - \frac{\tilde{c}_k \left(\tilde{\mathbf{a}}_k^T,\, \tilde{b}_k\right)}{|I_{k_+}|} \right\| \\
&= \sum_{k \in C_+} \sum_{i \in I_{k_+}} \left\| c_i \left(\mathbf{a}_i^T,\, b_i\right) - \frac{c_i \left(\mathbf{a}_i^T,\, b_i\right) + \varepsilon_i}{|I_{k_+}|} \right\| \\
&\leq \sum_{k \in C_+} \sum_{i \in I_{k_+}} \left[\left(1 - \frac{1}{|I_{k_+}|}\right) |c_i| \left\| \left(\mathbf{a}_i^T,\, b_i\right) \right\| + \frac{\|\varepsilon_i\|}{|I_{k_+}|} \right] \\
&\leq |C_+| \cdot \delta_{\max} + \left(1 - \frac{1}{N_{\max}}\right) \sum_{i \in I_+} |c_i| \left\| \left(\mathbf{a}_i^T,\, b_i\right) \right\|
\end{aligned}
$$

where we denote by I_{k+} the set of indices $i \in I_+$ that belong to the center $k \in C_+$ and $\varepsilon_i = \tilde{c}_k \left(\tilde{\mathbf{a}}_k^T,\, \tilde{b}_k\right) - c_i \left(\mathbf{a}_i^T,\, b_i\right)$ is the vector of the difference of the $i-$th generator, with its corresponding K-means cluster center.

The maximum value of the upper bound occurs when I_+ contains all indices that correspond to $c_i > 0$. This value gives us an upper bound for $\max_{\mathbf{u} \in P} d(\mathbf{u}, \tilde{P})$. To compute an upper bound for $\max_{\mathbf{v} \in \mathcal{V}_{\tilde{P}}} d(P, \mathbf{v})$ we assume $\mathbf{v} = \sum_{k \in C_+} \tilde{c}_k \left(\tilde{\mathbf{a}}_k^T \quad \tilde{b}_k\right)$ and consider the vertex $\sum_{i \in I_+} c_i \left(\mathbf{a}_i^T,\, b_i\right) \in P$ where I_+ is the set of indices of positive generators corresponding to the union of all clusters corresponding to the centers of C_+. Note that the occurring distance

$$
\left\| \sum_{i \in I_+} c_i \left(\mathbf{a}_i^T,\, b_i\right) - \sum_{k \in C_+} \tilde{c}_k \left(\tilde{\mathbf{a}}_i^T,\, \tilde{b}_i\right) \right\|
$$

was taken into account when computing the upper bound for $\max_{\mathbf{u} \in \mathcal{V}_P} d(\mathbf{u}, \tilde{P})$, and thus both values obtain the same upper bound. Therefore,

$$
\mathcal{H}\left(P, \tilde{P}\right) \leq K_+ \cdot \delta_{\max} + \left(1 - \frac{1}{N_{\max}}\right) \sum_{i \in I_+} |c_i| \left\| \left(\mathbf{a}_i^T,\, b_i\right) \right\|
$$

where K_+ is the number of cluster centers corresponding to $\tilde{P}$ and I_+ the indices corresponding to all positive generators of P. Similarly,

$$
\mathcal{H}\left(Q, \tilde{Q}\right) \leq K_- \cdot \delta_{\max} + \left(1 - \frac{1}{N_{\max}}\right) \sum_{i \in I_-} |c_i| \left\| \left(\mathbf{a}_i^T,\, b_i\right) \right\|
$$

where K_-, I_- are defined in analogous way for the negative zonotope. Combining the relations gives the desired bound.

$$
\frac{1}{\rho} \cdot |v(\mathbf{x}) - \tilde{v}(\mathbf{x})| \leq \mathcal{H}\left(P, \tilde{P}\right) + \mathcal{H}\left(Q, \tilde{Q}\right) \leq K \cdot \delta_{\max} + \left(1 - \frac{1}{N_{\max}}\right) \sum_{i=1}^{n} |c_i| \left\| \left(\mathbf{a}_i^T,\, b_i\right) \right\|
$$

□

C.3 ILLUSTRATION FOR NEURAL PATH K-MEANS ALGORITHM

Below we illustrate the vectors on which K-means is applied for the multi-output case. The vectors that are compressed are consist of all the edges associated to a hidden layer neuron. The corresponding edges contain all the possible neural paths that begin from some node of the input, end in some node of the output and pass through this hidden node.

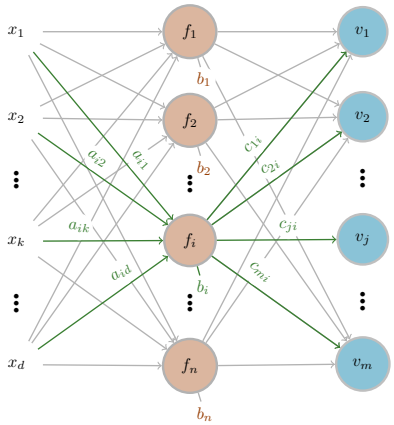

Figure 6: Neural Path K-means for multi-output neural network compression. In green color we highlight the weights corresponding to the $i-$th vector used by Neural Path K-means.

In the main text we defined the null generators of zonotopes that occur by the execution of Neural Path K-means. Below we provide an illustration for them.

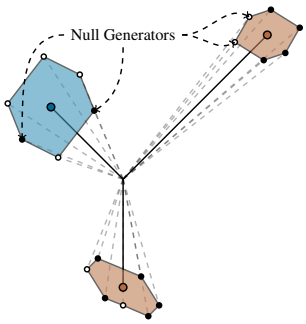

Figure 7: Visualization of K-means in $\mathbb{R}^{d+1+n}$, where d is the input dimension and n the hidden layer size. We color points according to the $j-$th output component of the network. Black and white points correspond to generators of P_j and Q_j respectively. White vertices in positive (brown) clusters and black vertices in negative (blue) clusters are null generators regarding $j-$th output.

C.4 PROOF OF PROPOSITION 6

Proof. Let us first focus on a single output, say $j-$th output. As in the proof for Zonotope K-means, we will bound $\mathcal{H}\left(P_j, \tilde{P}_j\right), \mathcal{H}\left(Q_j, \tilde{Q}_j\right)$ for all $j \in [m]$. From triangle inequality we get

$$|v_j(\mathbf{x}) - \tilde{v}_j(\mathbf{x})| \leq |p_j(\mathbf{x}) - \tilde{p}_j(\mathbf{x})| + |q_j(\mathbf{x}) - \tilde{q}_j(\mathbf{x})|$$

Any vertex of $\mathbf{u} \in P_j$ can be written as $\mathbf{u} = \sum_{i \in I_{j+}} c_{ji} \left(\mathbf{a}_i^T, b_i\right)$ where the set of indices I_{j+} satisfy $c_{ji} > 0$, $\forall i \in I_{j+}$ and thus correspond to positive generators. To choose a nearby vertex from $\tilde{P}_j$ we perform the following. For each $i \in I_{j+}$ we select the center $\left(\tilde{\mathbf{a}}_k^T \quad \tilde{b}_k \quad \tilde{C}^{(k)T}\right)$ of the cluster to where $\left(\mathbf{a}_i^T \quad b_i \quad C^{(i)T}\right)$ belongs, only if $\tilde{c}_{jk} > 0$. Such a center only exists if $c_{ji} \left(\mathbf{a}_i^T, b_i\right)$ is not a

null generator. Else, we choose as representation the vector $\mathbf{0}$. Each cluster center, or $\mathbf{0}$, is taken into account once and the vertex $\sum_{k\in C_{j+}} \tilde{c}_{jk}\left(\tilde{\mathbf{a}}_k,\, \tilde{b}_k\right) \in \tilde{P}_j$ is formed. We derive:

$$
\begin{aligned}
\max_{u\in\mathcal{V}_{P_j}} \operatorname{dist}\left(u, \tilde{P}_j\right) &\leq \left\| \sum_{i\in I_{j+}} c_{ji}\left(\mathbf{a}_i^T,\, b_i\right) - \sum_{k\in C_{j+}} \tilde{c}_{jk}\left(\tilde{\mathbf{a}}_k^T,\, \tilde{b}_k\right) \right\| \\
&\leq \sum_{k\in C_{j+}} \left\| \sum_{i\in I_{jk+}} c_{ji}\left(\mathbf{a}_i^T,\, b_i\right) - \tilde{c}_{jk}\left(\tilde{\mathbf{a}}_k^T,\, \tilde{b}_k\right) \right\| + \sum_{i\in N_{j+}} |c_{ji}| \left\|\left(\mathbf{a}_i^T,\, b_i\right)\right\| \\
&\leq \sum_{k\in C_{j+}} \sum_{i\in I_{jk+}} \left\| c_{ji}\left(\mathbf{a}_i^T,\, b_i\right) - \frac{\tilde{c}_{jk}\left(\tilde{\mathbf{a}}_k^T,\, \tilde{b}_k\right)}{|I_{jk+}|} \right\| + \sum_{i\in N_{j+}} |c_{ji}| \left\|\left(\mathbf{a}_i^T,\, b_i\right)\right\| \\
&\leq \sum_{k\in C} \sum_{i\in I_{jk+}} \left\| c_{ji}\left(\mathbf{a}_i^T,\, b_i\right) - \frac{(c_{ji}+\varepsilon_{ji})\left[\left(\mathbf{a}_i^T,\, b_i\right) + \lambda_i\right]}{|I_{jk+}|} \right\| + \sum_{i\in N_{j+}} |c_{ji}| \left\|\left(\mathbf{a}_i^T,\, b_i\right)\right\| \\
&\leq \sum_{k\in C_{j+}} \sum_{i\in I_{jk+}} \left[\frac{|\varepsilon_{ji}|\|\lambda_i\|}{|I_{jk+}|} + \left(1 - \frac{1}{|I_{jk+}|}\right) |c_{ji}| \left\|\left(\mathbf{a}_i^T,\, b_i\right)\right\| \right] + \\
&+ \sum_{k\in C_{j+}} \sum_{i\in I_{jk+}} \left[\frac{|\varepsilon_{ji}| \left\|\left(\mathbf{a}_i^T,\, b_i\right)\right\| + |c_{ji}|\,\|\lambda_i\|}{|I_{jk+}|} \right] + \sum_{i\in N_{j+}} |c_{ji}| \left\|\left(\mathbf{a}_i^T,\, b_i\right)\right\|
\end{aligned}
$$

where for all $i \in I_{jk+}$ the $i-$th vector of K-means is represented by the $k-$th center $k \in C_{j+}$. We also assumed $\tilde{C}^{(i)} = C_{:,i} + \varepsilon^{(i)} \Rightarrow \tilde{c}_{ji} = c_{ji} + \varepsilon_{ji}$ and $\left(\tilde{\mathbf{a}}_i^T,\, \tilde{b}_i\right) = \left(\mathbf{a}_i^T,\, b_i\right) + \lambda_i$.

The maximum value of the upper bound occurs when I_{j+} contains all indices that correspond to $c_{ji} > 0$. To compute an upper bound for $\max_{\mathbf{v}\in\mathcal{V}_{\tilde{P}_j}} \operatorname{dist}\left(P_j, \mathbf{v}\right)$ we write the vertex $\mathbf{v}$ as $\mathbf{v} = \sum_{k\in C_{j+}} \tilde{c}_{jk}\left(\tilde{\mathbf{a}}_k^T \quad \tilde{b}_k\right) \in \tilde{P}_j$ and choose the vertex $\mathbf{u} = \sum_{i\in I_{j+}} c_{ji}\left(\mathbf{a}_i^T,\, b_i\right)$ of P_j where I_{j+} is the set of all indices corresponding to generators that belong to these clusters. As in the proof of Proposition 5, their distance was taken into account when computing the upper bound for $\max_{\mathbf{u}\in\mathcal{V}_{P_j}} \operatorname{dist}\left(\mathbf{u}, \tilde{P}_j\right)$. Hence, both obtain the same upper bound which leads to

$$
\begin{aligned}
\mathcal{H}\left(P_j, \tilde{P}_j\right) \leq &\sum_{k\in C_{j+}} \sum_{i\in I_{jk+}} \left[\frac{|\varepsilon_{ji}|\|\lambda_i\|}{|I_{jk+}|} + \left(1 - \frac{1}{|I_{jk+}|}\right) |c_{ji}| \left\|\left(\mathbf{a}_i^T,\, b_i\right)\right\| \right] + \\
&+ \sum_{k\in C_{j+}} \sum_{i\in I_{jk+}} \left[\frac{|\varepsilon_{ji}| \left\|\left(\mathbf{a}_i^T,\, b_i\right)\right\| + |c_{ji}|\,\|\lambda_i\|}{|I_{jk+}|} \right] + \sum_{i\in N_{j+}} |c_{ji}| \left\|\left(\mathbf{a}_i^T,\, b_i\right)\right\|
\end{aligned}
$$

where I_{j+} contains all indices corresponding to positive c_{ji}. Similarly, we deduce

$$
\begin{aligned}
\mathcal{H}\left(Q_j, \tilde{Q}_j\right) \leq &\sum_{k\in C_{j-}} \sum_{i\in I_{jk-}} \left[\frac{|\varepsilon_{ji}|\|\lambda_i\|}{|I_{jk-}|} + \left(1 - \frac{1}{|I_{jk-}|}\right) |c_{ji}| \left\|\left(\mathbf{a}_i^T,\, b_i\right)\right\| \right] + \\
&+ \sum_{k\in C_{j-}} \sum_{i\in I_{jk-}} \left[\frac{|\varepsilon_{ji}| \left\|\left(\mathbf{a}_i^T,\, b_i\right)\right\| |c_{ji}|\,\|\lambda_i\|}{|I_{jk-}|} \right] + \sum_{i\in N_{j-}} |c_{ji}| \left\|\left(\mathbf{a}_i^T,\, b_i\right)\right\|
\end{aligned}
$$

where I_{j-} contains all i such that $c_{ji} < 0$. In total these bounds together with Proposition 4 give

$$\frac{1}{\rho}\cdot\max_{\mathbf{x}\in\mathcal{B}}|v_j(\mathbf{x})-\tilde{v}_j(\mathbf{x})|\leq\sum_{k\in C_j}\sum_{i\in I_{jk}}\left[\frac{|\varepsilon_{ji}|\|\lambda_i\|}{|I_{jk}|}+\left(1-\frac{1}{|I_{jk}|}\right)|c_{ji}|\left\|\left(\mathbf{a}_i^T,\,b_i\right)\right\|\right]+$$
$$+\sum_{k\in C_j}\sum_{i\in I_{jk}}\left[\frac{|\varepsilon_{ji}|\left\|\left(\mathbf{a}_i^T,\,b_i\right)\right\|+|c_{ji}|\,\|\lambda_i\|}{|I_{jk}|}\right]+\sum_{i\in N_j}|c_{ji}|\left\|\left(\mathbf{a}_i^T,\,b_i\right)\right\|$$

Here we used the notation $C_j=C_{j+}\cup C_{j-}=\{1,2,...,K\}$ and I_{jk} is either equal to I_{jk+} or I_{jk-} depending on $k\in C_j$. Note that $\{i|i\in I_{jk},k\in C_j\}=\{1,2,...,n\}\setminus N_j\subseteq\{1,2,...,n\}$, since every generator that is not null corresponds to some cluster center with the same sign. Also, using $N_{\text{max}}\geq|I_{jk}|\geq N_{\text{min}}$, it follows that

$$\frac{1}{\rho}\cdot\max_{\mathbf{x}\in\mathcal{B}}|v_j(\mathbf{x})-\tilde{v}_j(\mathbf{x})|\leq\sum_{i=1}^{n}\left[\frac{|\varepsilon_{ji}|\|\lambda_i\|}{N_{\text{min}}}+\left(1-\frac{1}{N_{\text{max}}}\right)|c_{ji}|\left\|\left(\mathbf{a}_i^T,\,b_i\right)\right\|\right]+$$
$$+\sum_{i=1}^{n}\left[\frac{|\varepsilon_{ji}|\left\|\left(\mathbf{a}_i^T,\,b_i\right)\right\|+|c_{ji}|\,\|\lambda_i\|}{N_{\text{min}}}\right]+\sum_{i\in N_j}|c_{ji}|\left\|\left(\mathbf{a}_i^T,\,b_i\right)\right\|$$

We will compute the total cost that combines all outputs by applying the inequality

$$\left(\sum_{j=1}^{m}|u_j|\right)^2\leq m\left(\sum_{j=1}^{m}|u_j|^2\right)\Leftrightarrow\sum_{j=1}^{m}|u_j|\leq\sqrt{m}\,\|(u_1,...,u_m)\|$$

which is a direct application of Cauchy-Schwartz inequality. Together with the relations $\|\varepsilon^{(i)}\|<\delta_{\text{max}},\quad\|\lambda_i\|<\delta_{\text{max}}$, we get

$$\frac{1}{\rho}\cdot\sum_{j=1}^{m}\max_{\mathbf{x}\in\mathcal{B}}|v_j(\mathbf{x})-\tilde{v}_j(\mathbf{x})|\leq\sum_{j=1}^{m}\sum_{i=1}^{n}\left[\frac{|\varepsilon_{ji}|\|\lambda_i\|}{N_{\text{min}}}+\left(1-\frac{1}{N_{\text{max}}}\right)|c_{ji}|\left\|\left(\mathbf{a}_i^T,\,b_i\right)\right\|\right]+$$
$$+\sum_{j=1}^{m}\sum_{i=1}^{n}\left[\frac{|\varepsilon_{ji}|\left\|\left(\mathbf{a}_i^T,\,b_i\right)\right\|+|c_{ji}|\,\|\lambda_i\|}{N_{\text{min}}}\right]+\sum_{j=1}^{m}\sum_{i\in N_j}|c_{ji}|\left\|\left(\mathbf{a}_i^T,\,b_i\right)\right\|$$

$$\leq\sum_{i=1}^{n}\left[\frac{\sqrt{m}\left\|\varepsilon^{(i)}\right\|\|\lambda_i\|}{N_{\text{min}}}+\left(1-\frac{1}{N_{\text{max}}}\right)\sqrt{m}\,\|C_{:,i}\|\left\|\left(\mathbf{a}_i^T,\,b_i\right)\right\|\right]+$$
$$+\sum_{i=1}^{n}\left[\frac{\sqrt{m}\left\|\varepsilon^{(i)}\right\|\left\|\left(\mathbf{a}_i^T,\,b_i\right)\right\|+\sqrt{m}\,\|C_{:,i}\|\,\|\lambda_i\|}{N_{\text{min}}}\right]+\sum_{j=1}^{m}\sum_{i\in N_j}|c_{ji}|\left\|\left(\mathbf{a}_i^T,\,b_i\right)\right\|$$
$$\leq\sqrt{m}K\delta_{\text{max}}^2+\sqrt{m}\left(1-\frac{1}{N_{\text{max}}}\right)\sum_{i=1}^{n}\|C_{:,i}\|\left\|\left(\mathbf{a}_i^T,\,b_i\right)\right\|+$$
$$\frac{\sqrt{m}\delta_{\text{max}}}{N_{\text{min}}}\sum_{i=1}^{n}\left(\left\|\left(\mathbf{a}_i^T,\,b_i\right)\right\|+\|C_{:,i}\|\right)+\sum_{j=1}^{m}\sum_{i\in N_j}|c_{ji}|\left\|\left(\mathbf{a}_i^T,\,b_i\right)\right\|$$

as desired. □

D EXPERIMENTAL SPECIFICATIONS

Experimental Setup For our code's execution we used Google's Colab GPU machines.

Training specifications Small CNNs such as the custom CNNs from Smyrnis et al. (2020); Smyrnis & Maragos (2020) and LeNet5 LeCun et al. (1998) were trained using Adam optimizer with learning rate 10^{-3} for 20 epochs. Larger CNNs CIFAR-VGG and modified AlexNet were trained with frozen

convolutional layers with SGD at learning rate 10^{-2}, momentum 0.9 and weight decay $5 \cdot 10^{-4}$ for 28 epochs. For each experiment we train from start 5 distinct models. The reported accuracy percentages are taken as the average across these 5 models. Standard deviation is provided both for tabular reports and on figure plots as error bars.

Pruning specifications Our algorithms are not deterministic, since K-means has random initialization. To ensure better performance each algorithm was repeated multiple times and the pruned model with the best validation accuracy was provided as output. In particular, we repeat each algorithm's execution 20 on the experiment of comparison to Smyrnis & Maragos (2020), 1 for the CIFAR experiment, and 5 for the rest of the experiments.